

---

# NaLaFormer: Norm-Aware Linear Attention for Transformer Models

---

Weikang Meng<sup>1,2</sup> Yadan Luo<sup>3</sup> Liangyu Huo<sup>1</sup> Yaowei Wang<sup>1,2</sup>  
Xin Li<sup>2</sup> Zheng Zhang<sup>1\*</sup>

<sup>1</sup>Harbin Institute of Technology, Shenzhen, China

<sup>2</sup>Pengcheng Laboratory, China

<sup>3</sup>UQMM Lab, University of Queensland, Australia

{zacharymengwk, huoliangyu1126, darrenzz219}@gmail.com

## Abstract

Linear attention has emerged as a viable alternative to softmax attention by reducing complexity from quadratic to linear in sequence length. To preserve two fundamental properties of softmax, non-negativity and entropy reduction, current works employ various linearly separable kernel functions with  $L1$  normalization instead of softmax operator. However, query norms are neglected by the normalization operation in linear attention, such degradation heavily leads to an entropy gap. Meanwhile, existing works inhibit negative values of query and key vectors resulting in a missing inner-product interactions after being mapped. To address these dual challenges, we propose a novel Norm-Aware Linear Attention mechanism serving to restore norm-guided dynamic spikiness and recover kernel-perturbed norm distributions. Specifically, we first decouple query and key matrices into two components: norm and direction, to achieve norm-aware spikiness control and norm consistency, respectively. We mathematically reveal that the extent of entropy reduction varies with the query norm in softmax normalization, motivating a query-norm aware kernel function for dynamic control over entropy reduction. Furthermore, to ensure norm consistency and enforce non-negativity constraints, we employ a norm-preserving mapping to project all elements of the angular matrix into positive values, leveraging cosine similarity to inhibit dimensions with opposite directions. We conduct extensive experiments demonstrating that the NaLaFormer improves performance on vision and language tasks, enhancing both expressiveness and efficiency by up to 4.2%.

## 1 Introduction

Transformer models [1, 2] have demonstrated remarkable success in both vision and language tasks. The core self-attention mechanism models global contextual relationships through softmax-normalized dot-product similarity, but incurs quadratic complexity  $\mathcal{O}(N^2)$  relative to sequence length  $N$ , creating significant computational overhead for long sequences or high-resolution images. To address this limitation, linear attention [3, 4, 5, 6, 7] replaces the  $\exp(\cdot)$  operator in softmax with a linearly separable kernel  $\phi(\cdot)$ . This reformulation reorders computation priorities from  $\exp(\mathbf{q}_i \mathbf{k}_j^\top) \mathbf{v}_j$  to  $\phi(\mathbf{q}_i)(\phi(\mathbf{k}_j)^\top \mathbf{v}_j)$  achieving linear complexity  $\mathcal{O}(N)$  through associative matrix multiplication.

Although linear attention mechanisms have gained popularity for their efficiency in sequence modeling, yet they consistently *underperform* compared to their softmax-based counterparts. A central limitation lies in the restricted expressiveness of the kernel function  $\phi(\cdot)$ , which approximates attention through inner products of transformed queries and keys,  $\phi(\mathbf{q})^\top \phi(\mathbf{k}_i)$ . Early approaches

---

\*Corresponding author.

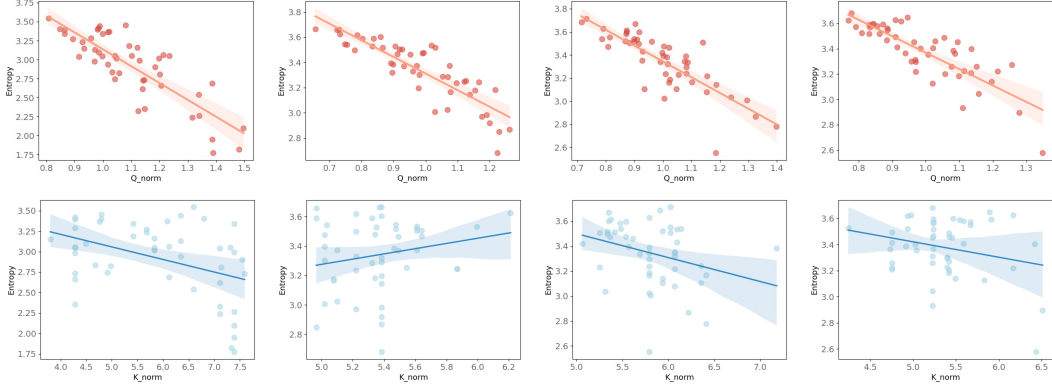


Figure 1: **Visualizations of correlation between entropy and vector norm.** We visualize two critical properties of the feature map: entropy and vector norms. The upper visualization correlates softmax-normalized feature map entropy ( $y$ -axis) with  $\mathbf{q}$  norms ( $x$ -axis), while the lower part visualizes the norm of  $\mathbf{k}$  with the greatest similarity.

focused on ensuring *non-negativity*, a necessary condition for interpreting attention scores as normalized distributions. To this end, various activation functions have been employed, including ReLU [5, 4],  $1 + \text{ELU}$  [3], and SiLU [8, 6], as well as positive-valued randomized feature mappings such as the Gaussian kernel  $\phi(x) = \exp(-|x|^2/2)$ . However, these kernels inherently discard negative components of the input, limiting their ability to capture the full range of semantic relationships.

As a result, linear attention often yields overly smooth attention distributions, lacking the *spikiness* characteristic of softmax attention. This leads to elevated entropy and hinders the model’s ability to focus on semantically critical tokens. Recent efforts such as Hedgehog [9], FLatten Transformer [5], and PolaFormer [10], attempt to address this shortcoming by introducing element-wise power functions to sharpen token-wise attention. While these methods empirically improve discrimination, the underlying cause of the entropy explosion in linear attention remains poorly understood.

To further explore the property of entropy, inspired by prior studies [11, 12, 13] that have identified the  $\mathbf{q}\mathbf{k}^\top$  norm cancellation in softmax attention, we notice that linear attention exhibits a different behavior, especially showing *asymmetric sensitivity* to the query and key norms. To analyze this effect, we employ a norm-direction decomposition of linear attention:

$$\text{LinearAttn}_t = \frac{\phi(\mathbf{q}_t) \sum_{i=1}^N \phi(\mathbf{k}_i)^\top \mathbf{v}_i}{\phi(\mathbf{q}_t) \sum_{j=1}^N \phi(\mathbf{k}_j)^\top} = \frac{\underbrace{\|\phi(\mathbf{q}_t)\|}_{\text{norm-unaware}} d(\phi(\mathbf{q}_t)) \sum_{i=1}^N \|\phi(\mathbf{k}_i)\| d(\phi(\mathbf{k}_i))^\top \mathbf{v}_i}{\|\phi(\mathbf{q}_t)\| d(\phi(\mathbf{q}_t)) \sum_{j=1}^N \|\phi(\mathbf{k}_j)\| d(\phi(\mathbf{k}_j))^\top}. \quad (1)$$

where  $d(\mathbf{x}) = \mathbf{x} / \|\mathbf{x}\|$  refers to the direction component. Eq. (1) exposes a critical *asymmetry* where only *key norms* influence linear attention outputs, as *query norms* are reduced through normalization. To further test this conjecture, Fig. 1 demonstrates a strong inverse correlation between entropy and query norms in softmax attention, whereas key norms exhibit weak correlation with spikiness. Notably, current linear attention approaches utilize element-wise kernel functions to enforce non-negativity constraints, suffering from the norm degradation and negative values loss.

In this work, we establish a mathematical framework characterizing query norm-entropy control in softmax attention. Based on these insights, we propose **Norm-aware Linear Attention**, a novel mechanism that explicitly couples  $\|\phi(\mathbf{q}_t)\|$  with spikiness to address the limitation of the query norm unawareness in linear attention. Our theoretical analysis reveals the dynamic control of entropy reduction (spikiness) from  $\|\phi(\mathbf{q}_t)\|$ . Specifically, for each direction of  $\mathbf{q}_t$ , the entropy decreases with a great  $\|\mathbf{q}_t\|$  monotonically. Empirical validation through randomized sampling of attention computations (Fig. 1 and Fig. 2 (b)) demonstrates that the  $\|\mathbf{q}_t\|$  is practically great enough in most cases. To jointly preserve spikiness and norm awareness, we employ a power function for each  $\mathbf{q}_t$  with an adaptive query norm aware power.

To address norm degradation in conventional linear attention while preserving non-negativity constraints, we proposed a *cosine inhibit* algorithm to only map the direction component. Utilizing Ptolemy’s theorem as a geometric foundation, our method employs cosine similarity for dimensional rescaling, selectively suppressing dimensions with distant direction and keeping closed dimensions.

These synergistic innovations faithfully capture essential properties of softmax operators while maintaining computational efficiency. Extensive experiments across core vision tasks (image classification, object detection and segmentation) demonstrate consistent performance improvement up to 4.2%. Furthermore, we additionally train a 340M-language model from scratch and test on common-sense reasoning tasks, showing both higher accuracy and lower perplexity.

## 2 Preliminaries

In this section, we provide a brief introduction of norm-direction (ND) decomposition, and revisit softmax attention from a norm-aware perspective.

### 2.1 Norm-Direction (ND) Decomposition

Here, we give the definition of norm-direction decomposition with  $p$ -norm as follows:

**Definition 1** (ND Decomposition). *Let  $\mathbf{x} = (x_1, \dots, x_d) \in \mathbb{R}^d$  is a non-zero vector, then the ND decomposition of  $\mathbf{x}$  is defined by:*

$$\text{ND}(\mathbf{x}; p) = \|\mathbf{x}\|_p \cdot \mathbf{d}(\mathbf{x}), \text{ where } \mathbf{d}(\mathbf{x}) = \frac{(x_1, \dots, x_d)}{\|\mathbf{x}\|_p}.$$

We name  $\mathbf{d}(\mathbf{x})$  the direction components of vector  $\mathbf{x}$ . According to the Norm Equivalence Theorem [14], all norms on a finite-dimensional vector space are equivalent, thus we do not distinguish between different  $p$ -norm in the following discussions for simplicity.

### 2.2 Softmax Attention with ND Decomposition

Let  $\mathbf{X} \in \mathbb{R}^{N \times D}$  denote a sequence of  $N$  tokens with dimension  $D$ . We divide the dimension into  $h$  heads, and each single head has  $d$  dimensions. In a single head, the output  $\mathbf{O} = \{\mathbf{o}_t\}_{t=1}^N \in \mathbb{R}^{N \times d}$  is computed following:

$$\mathbf{O} = \text{Softmax}\left(\frac{\mathbf{Q}\mathbf{K}^\top}{\sqrt{d}}\right)\mathbf{V}, \quad \mathbf{o}_t = \frac{\sum_{i=1}^N \exp(\mathbf{q}_t \mathbf{k}_i^\top / \sqrt{d})}{\sum_{j=1}^N \exp(\mathbf{q}_t \mathbf{k}_j^\top / \sqrt{d})} \mathbf{v}_i, \quad (2)$$

in which  $\mathbf{Q}, \mathbf{K}, \mathbf{V} \in \mathbb{R}^{N \times d}$  denote query, key and value vectors respectively with  $N$  sequence length. The complexity of softmax attention is  $\mathcal{O}(N^2 d)$ . Then, we rewrite the Eq. (2) with the ND-decomposition, which shows a explicit relation to query and key norms.

$$\mathbf{o}_t = \sum_{i=1}^N \frac{\exp(\mathbf{q}_t \mathbf{k}_i^\top / \sqrt{d})}{\sum_{j=1}^N \exp(\mathbf{q}_t \mathbf{k}_j^\top / \sqrt{d})} \mathbf{v}_i = \sum_{i=1}^N \frac{\exp(\|\mathbf{q}_t\| \|\mathbf{k}_i\| \langle \mathbf{d}(\mathbf{q}_t), \mathbf{d}(\mathbf{k}_i) \rangle / \sqrt{d})}{\sum_{j=1}^N \exp(\|\mathbf{q}_t\| \|\mathbf{k}_j\| \langle \mathbf{d}(\mathbf{q}_t), \mathbf{d}(\mathbf{k}_j) \rangle / \sqrt{d})} \mathbf{v}_i. \quad (3)$$

Through the derivation of the norm-direction decomposition above, we notice that  $\|\mathbf{q}_t\|$  is not reduced in softmax normalization comparing with Eq. (1), indicating a critical property of softmax mechanism: the  $\|\mathbf{q}_t\|$  factor controls the attention weight explicitly.

## 3 Method

In this section, we present Norm-Aware Linear Attention (NaLaFormer), a novel attention mechanism designed to address two critical limitations of conventional linear attention frameworks, which introduces a dynamic control of entropy reduction with query norm awareness, to capture the query norm information neglected by linear attentions. In addition, our framework incorporates a cosine similarity-driven suppression mechanism to ensure the vector norm consistency in mapping and enforces non-negative constraints in  $\phi(\mathbf{q})\phi(\mathbf{k})^\top$ .

### 3.1 Query Norm-aware Attention

Linear attentions have been proposed [3] by designing a novel framework of the  $\mathbf{q}, \mathbf{k}$  similarity measure through linearly separable kernel functions followed with an  $L1$  normalization. Mathematically, the similarity in linear attention can be formulated as  $\text{SM}(\mathbf{q}, \mathbf{k}) = \phi(\mathbf{q})\phi(\mathbf{k})^\top$ , where the feature map  $\phi(\cdot) : \mathbb{R}^d \rightarrow \mathbb{R}^{d'}$  is applied to query & key vectors. Then, the output of linear attention can be written as,

$$\mathbf{o}_t = \sum_{i=1}^N \frac{\phi(\mathbf{q}_t)\phi(\mathbf{k}_i)^\top \mathbf{v}_i}{\sum_{j=1}^N \phi(\mathbf{q}_t)\phi(\mathbf{k}_j)^\top} = \frac{\phi(\mathbf{q}_t) \sum_{i=1}^N \phi(\mathbf{k}_i)^\top \mathbf{v}_i}{\phi(\mathbf{q}_t) \sum_{j=1}^N \phi(\mathbf{k}_j)^\top}. \quad (4)$$

Following the ND decomposition in softmax attention, we derive a linear attention mechanism as follows,

$$\text{LinearAttn}(\mathbf{q}, \mathbf{k}, \mathbf{v}; \phi) = \frac{\phi(\mathbf{q}_t) \sum_{i=1}^N \phi(\mathbf{k}_i)^\top \mathbf{v}_i}{\phi(\mathbf{q}_t) \sum_{j=1}^N \phi(\mathbf{k}_j)^\top}, \quad (5)$$

$$= \frac{\underbrace{\|\phi(\mathbf{q}_t)\|}_{\text{norm-unaware}} \text{d}(\phi(\mathbf{q}_t)) \sum_{i=1}^N \|\phi(\mathbf{k}_i)\| \text{d}(\phi(\mathbf{k}_i))^\top \mathbf{v}_i}{\underbrace{\|\phi(\mathbf{q}_t)\|}_{\text{norm-unaware}} \text{d}(\phi(\mathbf{q}_t)) \sum_{j=1}^N \|\phi(\mathbf{k}_j)\| \text{d}(\phi(\mathbf{k}_j))^\top} = \frac{\text{d}(\phi(\mathbf{q}_t)) \sum_{i=1}^N \|\phi(\mathbf{k}_i)\| \phi(\mathbf{k}_i)^\top \mathbf{v}_i}{\text{d}(\phi(\mathbf{q}_t)) \sum_{j=1}^N \|\phi(\mathbf{k}_j)\| \text{d}(\phi(\mathbf{k}_j))^\top}. \quad (6)$$

In Eq. (6), the  $\|\phi(\mathbf{q}_t)\|$  is cancelled by fraction reduction, causing a query norm unawareness in the linear attention mechanism. Motivated by this, our novel linear attention mechanism is to resolve this inherent limitation: The attention weight remains agnostic to the query norms of linear attention. Previous kernel functions in linear attentions are nearly linear transformations, *i.e.*,  $\phi(cx) \sim c \phi(x)$ , while some spiky norms like power function [10, 5] have a similar property that is  $\phi(cx) = c^p \phi(x)$ . Therefore, all these kernel norm separable kernel functions result in significant information loss because of query norm unawareness.

To investigate the operational dynamics of query norm in attention clearly, we introduce the positive sequence entropy (PSE) defined in PolaFormer [10] as,

**Definition 2** (Positive Sequence Entropy (PSE)). *Let a sequence  $\mathbf{x} = (x_1, \dots, x_N)$ , in which  $x_i \geq 0$ ,  $i = 1, \dots, N$ , and  $s = \sum_{i=1}^N x_i > 0$ . Then the entropy of this positive sequence is defined by:*

$$\text{PSE}(\mathbf{x}) = - \sum_{i=1}^N \frac{x_i}{s} \log\left(\frac{x_i}{s}\right), \quad s = \sum_{i=1}^N x_i. \quad (7)$$

PSE enables us to measure the information uncertainty of a similarity sequence  $\mathbf{q}\mathbf{k}_j^\top$  without normalization. Then, we provide an explanation of the entropy reduction function of the query norm using the following theorem.

**Theorem 1** (Query Norm Dynamic Entropy Reduction). *Let  $\mathbf{x} = (x_1, \dots, x_N)$  be a sequence, and let  $\Phi : (-\infty, +\infty) \mapsto [0, +\infty)$  be a spiky function serving to reduce the PSE through mapping each  $x_i$ . In the case  $\Phi(\cdot) = \exp(\cdot)$ , existing a constant value  $c_0$  satisfying: For  $c > c_0$ , we have*

$$\text{PSE}(\Phi(c\mathbf{x})) < \text{PSE}(\Phi(\mathbf{x})).$$

Full proof and supporting lemmas are provided in APPENDIX A.1.

In attention mechanism, we consider  $\mathbf{q}\mathbf{k}_i^\top$  as  $x_i$ , and  $c$  is the norm of  $\mathbf{q}$ . For those tokens with a greater query norm, the entropy tends to decrease. Theorem 1 reveals the roles of query norm that: In softmax attention, where  $x_i = \mathbf{q}\mathbf{k}_i^\top$ ,  $c = \|\mathbf{q}\|$ , existing a  $c_0$ , for  $c > c_0$ , PSE decreases with  $c$ . Consequently, query norms have a dynamic control on entropy reduction.

### 3.2 Kernel Function Design

In this section, we will introduce our kernel function. Based on Theorem 1, we have proved that the PSE reduction dynamically varies with query norm. Thus, our designed feature map needs to maintain two properties: non-negativity and query norm-aware spikiness.

**Query Norm Aware Kernel Function.** We first explore the constraints of the kernel function  $\Phi(\cdot)$  through the following theorem with the assumption that all elements in sequence  $\mathbf{x}$  is non-negative.

**Theorem 2** (Kernel Function Design). *Consider a positive sequence  $\mathbf{x} = (x_1, \dots, x_n)$ , calculated by  $\mathbf{q}\mathbf{k}_i^\top$ . Given a spiky function  $\Phi(\cdot)$  satisfying that  $\Phi : (-\infty, +\infty) \mapsto [0, +\infty)$  is a differentiable function with  $\Phi'(x) > 0$  and  $\Phi''(x) > 0$ . Then,  $\text{PSE}(\Phi(\cdot))$  is a decreasing function for a great query norm.*

Full proof and supporting lemmas are provided in APPENDIX A.1.

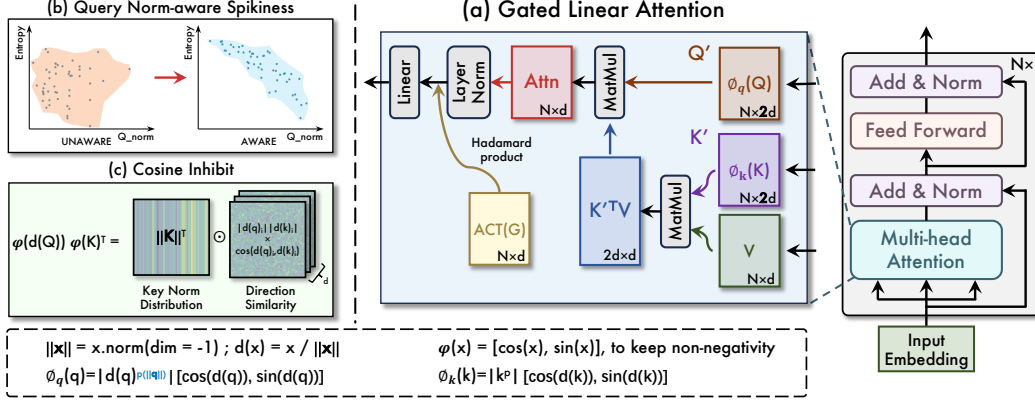


Figure 2: **The overall framework of NaLaFormer.** Our NaLaFormer block utilizes a simplified GLA [15] architecture (a), with a well-designed kernel function. (b) compares norm-aware vs. norm-unaware entropy distributions with query norm. The left half shows a random entropy distribution in linear attention (norm-unaware), while the right half exhibits Softmax normalization (norm-aware) inversely correlated with query norm. (c) demonstrates how cosine inhibit ensures the non-negativity.

Additionally, in linear attention,  $\Phi(\mathbf{q}\mathbf{k}^\top)$  must also be linear separatable, i.e.  $\Phi(\mathbf{q}\mathbf{k}^\top) = \phi(\mathbf{q})\phi(\mathbf{k})^\top$ . Thus, for simplicity and efficiency, we choose a dynamic query norm aware power function for queries and a fixed power function for keys. Additionally, to mitigate training instability and numerical overflow stemming from unbounded query norms, we deploy the  $\tanh(\cdot)$  activation as a bounded regularizer as follows:

$$p(x) = \lambda * (0.5 + \tanh(x)), \quad (8)$$

$$\Phi(\mathbf{q}\mathbf{k}_i^\top) = \phi_q(\mathbf{q})\phi_k(\mathbf{k}_i)^\top = \mathbf{d}(\mathbf{q})^{\text{p}(\|\mathbf{q}\|)} \mathbf{k}_i^{\lambda\top} = \|\mathbf{k}_i^\lambda\| \mathbf{d}(\mathbf{q})^{\text{p}(\|\mathbf{q}\|)} \mathbf{d}(\mathbf{k}_i^{\lambda\top}), \quad (9)$$

where  $\lambda$  is a hyperparameter to control the range of entropy. Therefore, the ND-decomposition of our kernel function can be written as,

$$\text{NaLaFormer}(\mathbf{q}, \mathbf{K}, \mathbf{V}; \Phi) = \frac{\sum_{i=1}^N \Phi(\mathbf{q}\mathbf{k}_i^\top) \mathbf{v}_i}{\sum_{i=1}^N \Phi(\mathbf{q}\mathbf{k}_i^\top)} = \frac{\sum_{i=1}^N \mathbf{d}(\mathbf{q})^{\text{p}(\|\mathbf{q}\|)} \mathbf{k}_i^{\lambda\top} \mathbf{v}_i}{\sum_{i=1}^N \mathbf{d}(\mathbf{q})^{\text{p}(\|\mathbf{q}\|)} \mathbf{k}_i^{\lambda\top}}, \quad (10)$$

$$= \frac{\sum_{i=1}^N \|\mathbf{k}_i^{\text{p}}\| \mathbf{d}(\mathbf{q})^{\text{p}(\|\mathbf{q}\|)} \mathbf{d}(\mathbf{k}_i^{\text{p}\top}) \mathbf{v}_i}{\sum_{i=1}^N \|\mathbf{k}_i^{\text{p}}\| \mathbf{d}(\mathbf{q})^{\text{p}(\|\mathbf{q}\|)} \mathbf{d}(\mathbf{k}_i^{\text{p}\top})}. \quad (11)$$

According to the Lemma 1 in PolaFormer [10], the composite function  $\Phi\mathbf{q}\mathbf{k}_i^\top$  with  $\Phi'(x) > 0$  and  $\Phi''(x) > 0$ . In addition, there is no cancellation on  $\|\mathbf{q}\|$ , and  $\Phi(\cdot)$  satisfying the condition in Theorem 1, indicating that our designed kernel function is a spiky function with query norm awareness.

**Keep Non-negative by Cosine Inhibit.** In previous work, to ensure all elements in the feature map remain positive, element-wise suppression of negative values in vectors was employed such as ReLU. However, these approaches lose information when computing inner products. In contrast, PolaFormer’s [10] sign-aware method decomposes a  $d$ -dimensional vector into  $4d$  dimensions, increasing computational overhead. To balance performance and efficiency, we investigate high-response query-key pairs in attention and computed their dimensional products. As shown in Fig. 3, we observe that only a few dimensions exhibit opposite signs (yielding negative products). Thus, it is feasible to only retain same-sign dimensions, and to maintain the norm, we suppress opposite-sign components via cosine inhibit as follows,

$$\varphi(\mathbf{d}(\mathbf{x})) = [\cos(\mathbf{d}(\mathbf{x})); \sin(\mathbf{d}(\mathbf{x}))], \mathbf{x} \in \mathbb{R}^d. \quad (12)$$

Due to the properties of the sine and cosine functions, we have  $\cos(x)^2 + \sin(x)^2 = 1$ , thus, this transformation is *norm-preserving*. To be more specific, the product of the direction  $\varphi(\mathbf{q})\varphi(\mathbf{k})^\top$  at dimension  $i$  is

$$\text{SM}_{\text{inhibit}}(\mathbf{d}(\mathbf{q}), \mathbf{d}(\mathbf{k}))_i \sim \varphi(\mathbf{d}(\mathbf{q}))_i \varphi(\mathbf{d}(\mathbf{k}))_i^\top, \quad (13)$$

$$= \cos(\mathbf{d}(\mathbf{q})_i) \cos(\mathbf{d}(\mathbf{k})_i) + \sin(\mathbf{d}(\mathbf{q})_i) \sin(\mathbf{d}(\mathbf{k})_i), \quad (14)$$

$$= \cos(\mathbf{d}(\mathbf{q})_i - \mathbf{d}(\mathbf{k})_i) > 0. \quad (15)$$

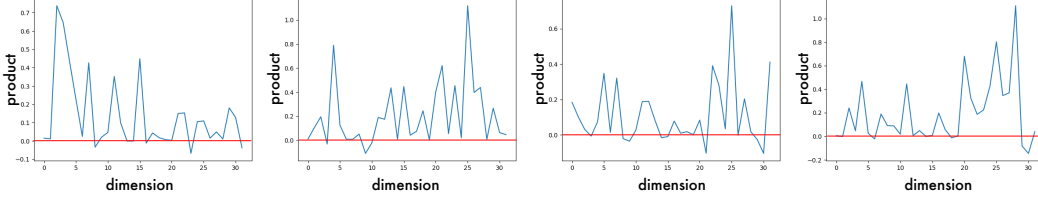


Figure 3: Visualization of the product of  $\mathbf{q}_d \mathbf{k}_d$  with the dimension, where the vector pair  $(\mathbf{q}, \mathbf{k})$  has the greatest similarity in one row of feature maps. Most dimensions have a positive (same-signed) product, thus the cosine inhibit will capture the product information of most dimensions.

Here, we map each elements of the direction components into  $[-\frac{\pi}{4}, \frac{\pi}{4}]$ , then  $(d(\mathbf{q})_i - d(\mathbf{k})_i) \in [-\frac{\pi}{2}, \frac{\pi}{2}]$  to keep the cosine inhibit positive. As shown in Fig. 2 (c), in each dimension, the cosine component in Eq. (13) when  $d(q_i)$  and  $d(k_i)$  are far away. Thus, the proposed method only inhibits the dimension with a different direction.

**Norm-Aware Linear Attention.** Now we combine the spiky function  $\phi(\cdot)$  with the non-negative function  $\varphi(\cdot)$ . Therefore, the overall summary of our kernel function is,

$$\phi_q(\mathbf{q}) = |\mathbf{d}(\mathbf{q})|^{\mathcal{P}(\|\mathbf{q}\|)} [\cos(d(\mathbf{q})); \sin(d(\mathbf{q}))], \quad \phi_k(\mathbf{k}) = |\mathbf{k}^\lambda| [\cos(d(\mathbf{k})); \sin(d(\mathbf{k}))], \quad (16)$$

$$\text{SM}(\mathbf{q}, \mathbf{k}) \sim \sum_{i=1}^d \|\mathbf{k}^\lambda\| \cdot |\mathbf{d}(\mathbf{q}^{\mathcal{P}(\|\mathbf{q}\|)})_i| |\mathbf{d}(\mathbf{k}^\lambda)_i| \underbrace{\cos(d(\mathbf{q})_i - d(\mathbf{k})_i)}_{\text{cosine-inhibit}}. \quad (17)$$

To validate the norm awareness of our proposed method, we additionally make a comparison of query norm vs. entropy among three cases, as shown in Fig. 4.

Finally, we utilize our norm-aware linear attention into gated linear attention [15, 16]. As shown in Fig. 2 (a), our norm-aware linear attention block consists of linear attention layer and feed forward network. After mapping query  $\mathbf{Q}$  and key  $\mathbf{K}$ , we first calculate  $\text{LinearAttn}(\phi_q(\mathbf{Q}), \phi_k(\mathbf{K}), \mathbf{V})$  in the multihead strategy, normalize the output through the LayerNorm operator, make the hadamard product with an activated gate matrix  $\mathbf{G}$ , and finally use a linear layer to integrate the output from different heads.

**Differences from Previous Works.** Previous works [17, 18] also keep part of the information with trigonometric functions. Cosformer [17] replaces the softmax in attention with a cosine-based distance metric, using cosine similarity to directly measure query-key alignment, while RoPE [18] encodes absolute positions via rotation matrices in complex space. However, both kinds of cosine similarity are employed for positional decay, which differs from our cosine inhibition method targeting dimensions with opposite signals, shown as follows:

$$\text{SM}_{\text{cosformer}}(\mathbf{q}_n, \mathbf{k}_m) = \phi(\mathbf{q}_n) \phi(\mathbf{k}_m)^\top \underbrace{\cos\left(\frac{(m-n)\pi}{2M}\right)}_{\text{relative position}}, \quad (18)$$

$$\text{SM}_{\text{rope}}(\mathbf{q}_n, \mathbf{k}_m) = \phi(\mathbf{q}_n) \underbrace{R_{\Theta, n-m}^d}_{\text{relative position}} \varphi(\mathbf{k}_m)^\top. \quad (19)$$

## 4 Experiments

In this section, we evaluate our **NaLaFormer** on both vision and language tasks. For vision tasks, we conduct experiments on image classification on ImageNet-1K [19], object detection & instance segmentation on COCO [20], and semantic segmentation on ADE20K [21], comparing the performance with current efficient models. In addition, we pre-train **NaLaFormer** language models from scratch and evaluate the pretrained model on common-sense reasoning tasks. All experiments were conducted on 8 NVIDIA A100, A800, A6000 and 3090 GPUs. Full experiment details are provided in APPENDIX A.2.

### 4.1 Image Classification on ImageNet-1K

**Settings.** We train **NaLaFormer** from scratch on ImageNet-1K [19] using Top-1 accuracy. For fairness, we categorized baseline models into 4 classes according to their parameter sizes and FLOPs, then make performance comparisons within each group.

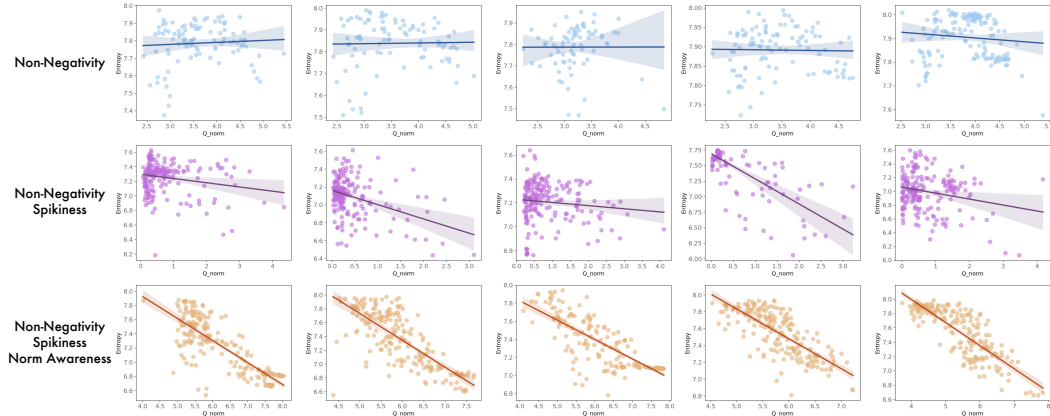


Figure 4: We visualize the query norm-entropy relationship under three approaches: (1) Only preserve non-negativity with 1 + ELU operator [3]. (2) Keep both non-negativity and spikiness with ReLU operator and power function as in FLatten [5]. (3) Introduce norm awareness property into spikiness (ours). There is a clear inverse correlation between entropy and query norms in ours approach.

**Results.** As shown in Table 1, our model consistently showing a higher accuracy comparing with the baseline models. For instance, our NaLaFormer-T obtains an increase from 3.8% to 7.5% compared with baseline linear models with comparable FLOPs. Additionally, under the setting of large size, the NaLaFormer-L consistently achieves a better performance compared with CNN, SSM and Transformer models. Notably, our model surpasses VRWKV-B [22] over 3.7% with fewer FLOPs. These results demonstrate our NaLaFormer improves the expressive capability of the attention mechanisms through replacing the standard attention.

Table 1: Comparison of the ImageNet-1K classification with the SOTA. The ‘‘Type’’ column specifies the architecture used: CNN represents convolutional neural networks, Trans for standard transformer, SSM for state space model, and Linear for linear attention.

MODEL	TYPE	PARA	FLOPS	ACC	MODEL	TYPE	PARA	FLOPS	ACC
VAN-b1 [23] (CVMI2023)	CNN	14M	2.5G	81.1	MambaOut-S [31] (CVPR2025)	CNN	49M	9.0G	84.1
Conv2Former-N [24] (TPAMI2024)	CNN	15M	2.2G	81.5	MogaNet-B [32] (ICLR2024)	CNN	44M	9.9G	84.3
PlainMamba-L1 [25] (BMVC2024)	SSM	7M	3.0G	77.9	VMamba-S [35] (NIPS2024)	SSM	50M	8.7G	83.6
PVT-T [26] (ICCV2021)	Trans	13M	1.9G	75.1	CSwin-S [37] (CVPR2022)	Trans	35M	7.0G	83.6
SBCFormer-L [27] (WACV2024)	Trans	19M	2.7G	81.1	PVTv2-b3 [41] (CVM2022)	Trans	45M	7.9G	83.2
RMT-T [28] (CVCR2024)	Trans	14M	2.5G	82.4	StructViT-B-8-1 [42] (CVPR2024)	Trans	52M	12.0G	84.3
FLattn-PVT-T [5] (ICCV2023)	Linear	11M	1.9G	77.8	SOFT-L [7] (ICV2024)	Linear	64M	11.0G	83.1
Agent-PVT-T [29] (ECCV2024)	Linear	12M	2.0G	78.4	FLattn-Swin-S [5] (ICCV2023)	Linear	51M	8.7G	83.5
ViG-T [30] (AAAI2025)	Linear	6M	0.9G	77.2	Agent-Swin-S [29] (ECCV2024)	Linear	50M	8.7G	83.7
VRWKV-T [22] (ICLR2025)	Linear	6M	1.2G	75.1	Pola-Swin-S [10] (ICLR2025)	Linear	50M	8.7G	83.6
Pola-PVT-T [10] (ICLR2025)	Linear	12M	2.0G	78.8	MILA-S [40] (NIPS2024)	Linear	43M	7.3G	84.4
NaLaFormer-T	Linear	15M	2.7G	<b>82.6</b>	ViG-H-S [30] (AAAI2025)	Linear	50M	8.8G	83.8
Conv2Former-T [24] (TPAMI2024)	CNN	27M	4.4G	83.2	NaLaFormer-B	Linear	52M	11.8G	<b>85.2</b>
MambaOut-T [31] (CVPR2025)	CNN	27M	4.5G	82.7	InterImage-B [33] (CVPR2023)	CNN	97M	16.0G	84.9
MogaNet-S [32] (ICLR2024)	CNN	25M	5.0G	83.4	MambaOut-S [31] (CVPR2025)	CNN	85M	15.8G	84.2
InternImage-T [33] (CVPR2023)	CNN	30M	5.0G	83.5	Vim-B [34] (ICML2024)	SSM	98M	13.7G	81.9
Vim-S [34] (ICML2024)	SSM	26M	3.7G	80.6	VMamba-B [35] (NIPS2024)	SSM	89M	15.4G	83.9
VMamba-T [35] (NIPS2024)	SSM	30M	4.9G	82.6	Swin-B [43] (ICCV2021)	Trans	88M	15.4G	83.5
LocalVMamba-T [36] (Arxiv2024)	SSM	26M	5.7G	82.7	SG-Former-B [38] (ICCV2023)	Trans	78M	15.6G	84.7
CSwin-T [37] (CVPR2022)	Trans	23M	4.3G	82.7	FLattn-Swin-B [5] (ICCV2023)	Linear	89M	15.4G	83.8
SG-Former-S [38] (ICCV2023)	Trans	23M	4.8G	83.2	Agent-Swin-B [29] (ECCV2024)	Linear	88M	15.4G	84.0
MOAT-0 [39] (ICLR2023)	Trans	28M	5.7G	83.3	FLattn-CSwin-B [5] (ICCV2023)	Linear	75M	15.0G	84.5
FLattn-Swin-T [5] (ICCV2023)	Linear	29M	4.5G	82.1	Agent-CSwin-B [29] (ECCV2024)	Linear	73M	14.9G	84.7
Agent-Swin-T [29] (ECCV2024)	Linear	29M	4.5G	82.6	Pola-Swin-B [10] (ICLR2025)	Linear	88M	15.4G	83.8
Pola-Swin-T [10] (ICLR2025)	Linear	29M	4.5G	82.6	VRWKV-B [22] (ICLR2025)	Linear	94M	18.2G	82.0
VRWKV-S [22] (ICLR2025)	Linear	24M	4.6G	80.1	ViG-B [30] (AAAI2025)	Linear	89M	13.8G	82.6
ViG-H-T [30] (AAAI2025)	Linear	29M	4.5G	82.8	MILA-B [40] (NIPS2024)	Linear	96M	16.2G	85.3
MILA-T [40] (NIPS2024)	Linear	25M	4.2G	83.5	ViG-H-B [30] (AAAI2025)	Linear	89M	15.5G	84.2
NaLaFormer-S	Linear	26M	5.1G	<b>84.3</b>	NaLaFormer-L	Linear	95M	17.7G	<b>85.7</b>

## 4.2 Object Detection and Instance Segmentation on COCO

**Settings.** We further conducted comprehensive experiments on the object detection task using the COCO dataset [20]. To systematically evaluate architectural compatibility, we independently integrated NaLaFormer as the backbone architecture into three established detection frameworks: Mask R-CNN [44] and RetinaNet [45]. All experiments were conducted using ImageNet-1k pretrained weights following the evaluation strategy in FLatten Transformer [5].

Table 2: Object detection and instance segmentation results on the COCO dataset using two detector, RetinaNet with 1 × schedule and Mask R-CNN with 1 × schedule.

METHOD	TYPE	RETINANET 1 ×						MASK R-CNN 1 ×					
		AP <sup>b</sup>	AP <sub>50</sub> <sup>b</sup>	AP <sub>75</sub> <sup>b</sup>	AP <sub>S</sub> <sup>b</sup>	AP <sub>M</sub> <sup>b</sup>	AP <sub>L</sub> <sup>b</sup>	AP <sup>b</sup>	AP <sub>50</sub> <sup>b</sup>	AP <sub>75</sub> <sup>b</sup>	AP <sup>m</sup>	AP <sub>50</sub> <sup>m</sup>	AP <sub>75</sub> <sup>m</sup>
PVTv2-b1 [41] <sub>(CVM2022)</sub>	Trans	41.2	61.9	43.9	25.4	44.5	54.3	41.8	54.3	45.9	38.8	61.2	41.6
SBCFormer-L [27] <sub>(WACV2024)</sub>	Trans	41.1	62.3	43.3	24.7	44.3	56.0	-	-	-	-	-	-
MPViT-XS [46] <sub>(CVPR2022)</sub>	Trans	45.9	67.4	49.4	28.5	50.1	60.8	47.3	69.1	51.9	42.7	66.2	46.0
SOFT + + T [7] <sub>(IJCV2024)</sub>	Linear	41.9	62.7	44.7	27.8	45.4	55.6	41.2	63.7	44.7	38.2	61.0	41.0
FLatten-PVT-T [5] <sub>(ICCV2023)</sub>	Linear	-	-	-	-	-	-	38.2	61.6	41.9	37.0	57.6	39.0
Agent-PVT-T [29] <sub>(ECCV2024)</sub>	Linear	-	-	-	-	-	-	41.4	64.1	45.2	38.7	61.3	41.6
Pola-PVT-T [10] <sub>(ICLR2025)</sub>	Linear	40.0	60.7	42.3	25.0	43.6	52.9	40.4	62.4	43.9	37.4	59.4	40.3
NaLaFormer-T	Linear	<b>46.2</b>	<b>67.9</b>	<b>49.5</b>	<b>29.9</b>	<b>50.4</b>	<b>61.6</b>	<b>47.6</b>	<b>69.5</b>	<b>52.4</b>	<b>43.0</b>	<b>66.7</b>	<b>46.5</b>
InternImage-T [33] <sub>(CVPR2023)</sub>	CNN	-	-	-	-	-	-	47.2	69.0	52.1	42.5	66.1	45.8
MambaOut-T [33] <sub>(CVPR2025)</sub>	CNN	-	-	-	-	-	-	45.1	67.3	49.6	41.0	64.1	44.1
VMamba-T [35] <sub>(NIPS2024)</sub>	SSM	-	-	-	-	-	-	46.5	68.5	50.7	42.1	65.5	45.3
MPViT-S [46] <sub>(CVPR2022)</sub>	Trans	45.7	57.3	48.8	28.7	49.7	59.2	46.4	68.6	51.2	42.4	65.6	45.7
CMT-S [47] <sub>(CVPR2022)</sub>	Trans	44.3	65.5	47.5	27.1	48.3	59.1	44.6	66.8	48.9	40.7	63.9	43.4
Agent-Swin-T [29] <sub>(ECCV2024)</sub>	Linear	-	-	-	-	-	-	44.6	67.5	48.7	40.7	64.4	43.4
MILA-T [40] <sub>(NIPS2024)</sub>	Linear	-	-	-	-	-	-	46.8	69.5	51.5	42.1	66.4	45.0
Pola-PVT-S [10] <sub>(ICLR2025)</sub>	Linear	43.2	64.1	46.4	28.0	46.4	57.9	43.9	66.1	47.9	40.2	63.1	43.0
Pola-Swin-T [10] <sub>(ICLR2025)</sub>	Linear	-	-	-	-	-	-	44.8	67.6	49.1	40.5	64.1	43.5
MILA-T [40] <sub>(NIPS2024)</sub>	Linear	-	-	-	-	-	-	46.8	69.5	51.5	42.1	66.4	45.0
NaLaFormer-S	Linear	<b>47.2</b>	<b>68.0</b>	<b>50.7</b>	<b>29.0</b>	<b>51.3</b>	<b>63.3</b>	<b>49.5</b>	<b>71.2</b>	<b>54.3</b>	<b>44.2</b>	<b>68.1</b>	<b>47.8</b>

Table 3: Comparison on object detection and instance segmentation (left) and semantic segmentation (right). The left table shows the results on the COCO dataset using Mask R-CNN with 3× schedule. For semantic segmentation task (right) on the ADE20K dataset, we employ two types of encoders: S corresponds to Semantic FPN, and U refers to UperNet.

METHOD	TYPE	MASK R-CNN 3 ×						METHOD	SEMANTIC SEG mIoU(%)		
		AP <sup>b</sup>	AP <sub>50</sub> <sup>b</sup>	AP <sub>75</sub> <sup>b</sup>	AP <sup>m</sup>	AP <sub>50</sub> <sup>m</sup>	AP <sub>75</sub> <sup>m</sup>		TYPE	S	U
XCiT-T12/8 [48] <sub>(NIPS2021)</sub>	Trans	44.5	66.4	48.8	40.4	63.5	43.3	VAN-B1 [23] <sub>(CVM2023)</sub>	CNN	42.9	-
MPViT-T [46] <sub>(CVPR2022)</sub>	Trans	44.8	66.9	49.2	41.0	64.2	44.1	PVT-T [26] <sub>(ICCV2021)</sub>	Trans	35.7	-
NaLaFormer-T	Linear	<b>46.7</b>	<b>67.4</b>	<b>51.3</b>	<b>42.0</b>	<b>65.0</b>	<b>45.7</b>	Agent-PVT-T [29] <sub>(ECCV2024)</sub>	Linear	40.2	-
InternImage-T [33] <sub>(CVPR2023)</sub>	CNN	49.1	70.4	54.1	43.7	67.3	47.3	VRWKV-T [22] <sub>(ICLR2025)</sub>	Linear	-	43.3
Conv2Former-T [24] <sub>(TPAMI2024)</sub>	CNN	48.0	69.5	52.7	43.0	66.8	46.1	ViG-T [30] <sub>(AAAI2025)</sub>	Linear	-	43.8
NAT-T [49] <sub>(CVPR2023)</sub>	Trans	47.8	69.0	52.6	42.6	66.0	45.9	NaLaFormer-T	Linear	<b>45.4</b>	<b>46.9</b>
GC-ViT-T [50] <sub>(ICML2023)</sub>	Trans	47.8	69.0	52.6	42.6	66.0	45.9	MambaOut-T [33] <sub>(CVPR2025)</sub>	CNN	-	47.4
FLatten-Swin-T [5] <sub>(ICCV2023)</sub>	Linear	46.5	68.5	50.8	42.1	65.4	45.1	VMamba-T [35] <sub>(NIPS2024)</sub>	SSM	-	47.3
Agent-Swin-T [29] <sub>(ECCV2024)</sub>	Linear	47.3	69.5	51.9	42.7	66.4	46.2	Agent-Swin-T [29] <sub>(ECCV2024)</sub>	Linear	-	46.7
Pola-Swin-T [10] <sub>(ICLR2025)</sub>	Linear	47.0	68.9	51.5	42.3	66.0	45.8	Agent-PVT-S [29] <sub>(ECCV2024)</sub>	Linear	44.2	-
MILA-T [40] <sub>(NIPS2024)</sub>	Linear	48.8	71.0	53.6	43.8	68.0	46.8	VRWKV-S [22] <sub>(ICLR2025)</sub>	Linear	46.9	47.2
NaLaFormer-S	Linear	<b>49.7</b>	<b>70.5</b>	<b>54.7</b>	<b>44.3</b>	<b>68.0</b>	<b>48.0</b>	ViG-S [30] <sub>(AAAI2025)</sub>	Linear	-	47.9
								NaLaFormer-S	Linear	<b>48.0</b>	<b>48.5</b>

**Results.** We show the results in Table 2 and Table 3 (left), our model surpasses the other baseline models across various frameworks. For example, our NaLaFormer-T tested on Mask R-CNN detectors with "1 ×" schedule achieves 47.6 AP<sup>b</sup> and 43.0 AP<sup>m</sup>, outperforming some larger baselines, such as MILA [40] and PolaFormer [10].

### 4.3 Semantic Segmentation on ADE20K

**Settings.** In this section, we integrate our model into the semantic segmentation task on ADE20K [21] datasets. Specifically, we adopt our model with the ImageNet-1K pre-trained weight into the Semantic FPN (S) [51] and UperNet (U) [52] using mIoU as the evaluation metric.

**Results.** As shown in Table 3 (right), the results demonstrate a better performance in mIoU. Specifically, the NaLaFormer-S with UperNet achieves 48.5%, showing a 2.7% improvement compared to PolaFormer [10] and 0.6% compared to ViG-S [30].

### 4.4 Language Modeling

In this section, we conduct our experiments by training a 340M-NaLaFormer from scratch and test the language modeling perplexity and zero-shot performance of commonsense reasoning tasks.

**Settings.** We train our model from scratch with parameter sizes of 340M on 15B tokens with a batch size of 0.5M tokens and test it on common-sense reasoning tasks. Our method is integrated in DeltaNet [8] and Gated DeltaNet [53] by replacing SiLU(·) function with our NaLaFormer.

**Results.** As shown in Table 4, baselines such as deltanet [8] and gated deltanet [53] demonstrate a consistent performance gain across various language reasoning tasks. By equipping with the proposed kernel functions, our model consistently outperform deltanet and gated deltanet.

### 4.5 Efficiency Analysis

We visualize the efficiency comparison between the proposed NaLaFormer and other approaches with similar FLOPs as shown in Fig. 6. The results show that our model can achieve comparable

Table 4: Comparison on common-sense reasoning tasks. Our model shows a competitive performance and gains an consistent improvement in multiple sub-tasks and achieves the best average accuracy and lower perplexity.

MODEL	WIKI. ppl ↓	LMB. ppl ↓	PIQA. acc ↑	HELLA. acc <sub>n</sub> ↑	WINO. acc ↑	ARC <sub>e</sub> . acc ↑	ARC <sub>c</sub> . acc <sub>n</sub> ↑	AVG.
Transformer++	28.39	42.69	63.3	34.0	50.4	44.5	24.2	43.3
RetNet	32.33	49.19	63.5	33.5	52.5	44.5	23.4	43.5
Mamba	28.39	39.66	65.0	35.4	50.1	46.3	23.6	44.1
GLA	28.65	43.35	64.8	34.5	51.4	45.1	22.7	43.7
DeltaNet	29.08	50.87	63.6	33.6	51.7	46.0	23.0	43.6
NaLa+DN	<b>27.82</b>	<b>49.77</b>	<b>64.9</b>	<b>34.3</b>	<b>52.7</b>	<b>46.5</b>	<b>23.1</b>	<b>44.3<sub>+0.7</sub></b>
Gated DeltaNet	26.59	<b>31.67</b>	<b>65.8</b>	35.2	50.8	<b>46.0</b>	23.5	44.3
NaLa+GDN	<b>25.89</b>	32.32	65.6	<b>36.2</b>	<b>53.2</b>	45.4	<b>23.8</b>	<b>44.8<sub>+0.5</sub></b>

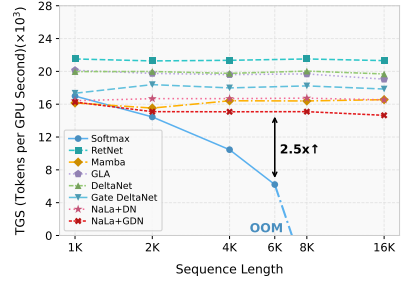


Figure 5: Comparison on training throughput of 340M models on a single A6000 GPU.

performance with significantly less computation. Furthermore, we present the training throughput comparison in Fig. 5. As the linear complexity of our proposed linear attention, our model achieves a competitive throughput compared with other baselines, and significantly faster than softmax attention.

#### 4.6 Ablation Study

**Impact of Components.** We evaluate the effectiveness of each component in NaLaFormer. In row 1, we keep non-negativity and spikiness with  $\text{ReLU}(\cdot)$  and a constant power function. In row 2, we utilize the cosine inhibit to additionally preserve the norm. In row 3, we replace the constant power with a norm aware power. As shown in Table 5, it is important to note that the norm awareness yields a 0.4% improvement in row 2 and row 3, indicating that norm-aware spikiness effectively capture the lost information due to the norm cancellation. We examine the impact of norm consistency with cosine inhibit in row 1 and row 2 by only preserving negative values, with our cosine inhibit, the information in negative values improves the performance 0.4%.

**Comparison with other Linear Attention.** To ensure fair comparison with existing linear attention approaches, we adopt the evaluation protocol from FLatten-Transformer [5] with Swin-T setting. As shown in Table 6, NaLaFormer achieves consistent performance gains across all baseline models, surpassing both conventional linear attention variants and softmax attention, while maintaining linear complexity.

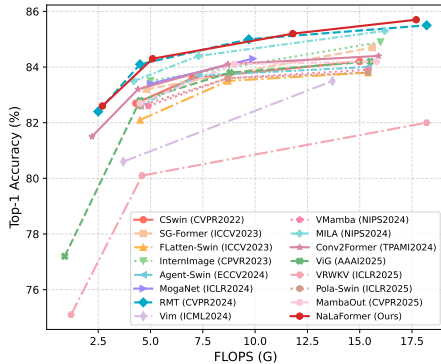


Figure 6: Efficiency analysis with Accuracy vs. FLOPs curves on the ImageNet-1K.

## 5 Conclusion

In this work, we presented NaLaFormer, a novel transformer model with linear attention. Our model is built on two properties of the standard softmax attention: (i) making the spikiness aware of query norm and (ii) non-negativity constraints. To fulfill these properties, we design a novel kernel function that explicitly incorporates the query norm into the power operation, enabling the entropy of attention weights reducing in query norm awareness; additionally, we utilize a cosine inhibit method to keep the feature map non-negative and avoid norm degradation. Besides, we mathematically prove the norm awareness of softmax attention and theoretically explain the design of NaLaFormer. We validated the effectiveness of the NaLaFormer in various vision tasks and pre-trained a 340M language model validated on common-sense reasoning tasks. The NaLaFormer achieves a better balance between performance and efficiency, demonstrating considerable potential for practical implementation.

Table 5: Ablation on the FL-Swin-T setting.

NON NEGATIVITY	SPIKY	NORM AWARE	NORM CONSISTENCY	ACC. (%)
✓	✓			82.1 <sub>-0.8</sub>
✓	✓		✓	82.5 <sub>-0.4</sub>
✓	✓	✓	✓	82.9

Table 6: Comparison with other linear attention models on the Swin-T setting.

METHOD	PARAMS	FLOPS	ACC(%)
Swin-T [43] (ICCV2021)	28M	4.4G	81.2
HydraAttn [54] (ECCV2022)	29M	4.5G	80.7
EfficientAttn [55] (WACV2021)	29M	4.5G	81.0
LinearAngular [56] (CVPR2023)	29M	4.5G	79.4
EnhancedAttn [4] (Arxiv2022)	29M	4.5G	81.8
FLattenAttn [5] (ICCV2023)	29M	4.5G	82.1
AgentAttn [29] (ECCV2024)	29M	4.5G	82.6
PolaFormer [10] (ICLR2025)	29M	4.5G	<b>82.6</b>
NaLaFormer	29M	4.8G	<b>82.9 (ours)</b>

## References

- [1] Ashish Vaswani, Noam Shazeer, Niki Parmar, Jakob Uszkoreit, Llion Jones, Aidan N. Gomez, Lukasz Kaiser, and Illia Polosukhin. Attention is all you need. In Proceedings of NeurIPS, pages 5998–6008, 2017.
- [2] Alexey Dosovitskiy, Lucas Beyer, Alexander Kolesnikov, Dirk Weissenborn, Xiaohua Zhai, Thomas Unterthiner, Mostafa Dehghani, Matthias Minderer, Georg Heigold, Sylvain Gelly, Jakob Uszkoreit, and Neil Houlsby. An image is worth 16x16 words: Transformers for image recognition at scale. In Proceedings of ICLR. OpenReview.net, 2021.
- [3] Angelos Katharopoulos, Apoorv Vyas, Nikolaos Pappas, and François Fleuret. Transformers are rns: Fast autoregressive transformers with linear attention. In Proceedings of ICML, volume 119, pages 5156–5165, 2020.
- [4] Han Cai, Chuang Gan, and Song Han. Efficientvit: Enhanced linear attention for high-resolution low-computation visual recognition. CoRR, abs/2205.14756, 2022.
- [5] Dongchen Han, Xuran Pan, Yizeng Han, Shiji Song, and Gao Huang. Flatten transformer: Vision transformer using focused linear attention. In Proceedings of IEEE ICCV, pages 5938–5948, 2023.
- [6] MiniMax, Aonian Li, Bangwei Gong, and et al. Minimax-01: Scaling foundation models with lightning attention. CoRR, abs/2501.08313, 2025.
- [7] Jiachen Lu, Junge Zhang, Xiatian Zhu, Jianfeng Feng, Tao Xiang, and Li Zhang. Softmax-free linear transformers. Int. J. Comput. Vis. (IJCV), 132(8):3355–3374, 2024.
- [8] Songlin Yang, Bailin Wang, Yu Zhang, Yikang Shen, and Yoon Kim. Parallelizing linear transformers with the delta rule over sequence length. In Proceedings of NeurIPS, 2024.
- [9] Michael Zhang, Kush Bhatia, Hermann Kumbong, and Christopher Ré. The hedgehog & the porcupine: Expressive linear attentions with softmax mimicry. In Proceedings of The 12th ICLR, 2024.
- [10] Weikang Meng, Yadan Luo, Xin Li, Dongmei Jiang, and Zheng Zhang. Polaformer: Polarity-aware linear attention for vision transformers. In Proceedings of ICLR, 2025.
- [11] Mostafa Dehghani, Josip Djolonga, and et al. Basil Mustafa. Scaling vision transformers to 22 billion parameters. In Proceedings of ICML, volume 202, pages 7480–7512, 2023.
- [12] Muzammal Naseer, Kanchana Ranasinghe, Salman Khan, Munawar Hayat, Fahad Shahbaz Khan, and Ming-Hsuan Yang. Intriguing properties of vision transformers. In Proceedings of NeurIPS, pages 23296–23308, 2021.
- [13] Maxim Milakov and Natalia Gimelshein. Online normalizer calculation for softmax. CoRR, abs/1805.02867, 2018.
- [14] Haim Brezis. Functional Analysis, Sobolev Spaces and Partial Differential Equations, volume 2. Springer, 2011.
- [15] Songlin Yang, Bailin Wang, Yikang Shen, Rameswar Panda, and Yoon Kim. Gated linear attention transformers with hardware-efficient training. In Proceedings of ICML, 2024.
- [16] Zhen Qin, Weigao Sun, Dong Li, Xuyang Shen, Weixuan Sun, and Yiran Zhong. Various lengths, constant speed: Efficient language modeling with lightning attention. In Proceedings of ICML, 2024.
- [17] Zhen Qin, Weixuan Sun, Hui Deng, Dongxu Li, Yunshen Wei, Baohong Lv, Junjie Yan, Lingpeng Kong, and Yiran Zhong. Cosformer: Rethinking softmax in attention. In Proceedings of The 10th ICLR, 2022.
- [18] Jianlin Su, Murtadha H. M. Ahmed, Yu Lu, Shengfeng Pan, Wen Bo, and Yunfeng Liu. Ro-former: Enhanced transformer with rotary position embedding. Neurocomputing, 568:127063, 2024.

- [19] Jia Deng, Wei Dong, Richard Socher, Li-Jia Li, Kai Li, and Li Fei-Fei. Imagenet: A large-scale hierarchical image database. In Proceedings of IEEE CVPR, pages 248–255, 2009.
- [20] Tsung-Yi Lin, Michael Maire, Serge J. Belongie, James Hays, Pietro Perona, Deva Ramanan, Piotr Dollár, and C. Lawrence Zitnick. Microsoft COCO: common objects in context. In Proceedings of ECCV, volume 8693, pages 740–755, 2014.
- [21] Bolei Zhou, Hang Zhao, Xavier Puig, Tete Xiao, Sanja Fidler, Adela Barriuso, and Antonio Torralba. Semantic understanding of scenes through the ADE20K dataset. IJCV, 127(3):302–321, 2019.
- [22] Yuchen Duan, Weiyun Wang, Zhe Chen, Xizhou Zhu, Lewei Lu, Tong Lu, Yu Qiao, Hongsheng Li, Jifeng Dai, and Wenhai Wang. Vision-rwkv: Efficient and scalable visual perception with rwkv-like architectures. In Proceedings of ICLR, 2025.
- [23] Meng-Hao Guo, Chengze Lu, Zheng-Ning Liu, Ming-Ming Cheng, and Shimin Hu. Visual attention network. CoRR, abs/2202.09741, 2022.
- [24] Qibin Hou, Cheng-Ze Lu, Ming-Ming Cheng, and Jiashi Feng. Conv2former: A simple transformer-style convnet for visual recognition. IEEE TAPMI, 46(12):8274–8283, 2024.
- [25] Chenhongyi Yang, Zehui Chen, Miguel Espinosa, Linus Ericsson, Zhenyu Wang, Jiaming Liu, and Elliot J. Crowley. Plainmamba: Improving non-hierarchical mamba in visual recognition. CoRR, abs/2403.17695, 2024.
- [26] Wenhai Wang, Enze Xie, Xiang Li, Deng-Ping Fan, Kaitao Song, Ding Liang, Tong Lu, Ping Luo, and Ling Shao. Pyramid vision transformer: A versatile backbone for dense prediction without convolutions. In Proceedings of IEEE ICCV, pages 548–558, 2021.
- [27] Xiangyong Lu, Masanori Suganuma, and Takayuki Okatani. Sbcformer: Lightweight network capable of full-size imagenet classification at 1 FPS on single board computers. In Proceedings of IEEE WACV, pages 1112–1122, 2024.
- [28] Qihang Fan, Huaibo Huang, Mingrui Chen, Hongmin Liu, and Ran He. RMT: retentive networks meet vision transformers. In Proceedings of IEEE CVPR, pages 5641–5651. IEEE, 2024.
- [29] Dongchen Han, Tianzhu Ye, Yizeng Han, Zhuofan Xia, Siyuan Pan, Pengfei Wan, Shiji Song, and Gao Huang. Agent attention: On the integration of softmax and linear attention. In Proceedings of ECCV, volume 15108, pages 124–140, 2024.
- [30] Bencheng Liao, Xinggang Wang, Lianghai Zhu, Qian Zhang, and Chang Huang. Vig: Linear-complexity visual sequence learning with gated linear attention. In Toby Walsh, Julie Shah, and Zico Kolter, editors, Proceedings of AAAI, pages 5182–5190, 2025.
- [31] Weihao Yu and Xinchao Wang. Mambaout: Do we really need mamba for vision? CoRR, abs/2405.07992, 2024.
- [32] Siyuan Li, Zedong Wang, Zicheng Liu, Cheng Tan, Haitao Lin, Di Wu, Zhiyuan Chen, Jiangbin Zheng, and Stan Z. Li. Moganet: Multi-order gated aggregation network. In Proceedings of ICLR, 2024.
- [33] Wenhai Wang, Jifeng Dai, Zhe Chen, Zhenhang Huang, Zhiqi Li, Xizhou Zhu, Xiaowei Hu, Tong Lu, Lewei Lu, Hongsheng Li, Xiaogang Wang, and Yu Qiao. Internimage: Exploring large-scale vision foundation models with deformable convolutions. In Proceedings of IEEE CVPR, pages 14408–14419, 2023.
- [34] Lianghai Zhu, Bencheng Liao, Qian Zhang, Xinlong Wang, Wenyu Liu, and Xinggang Wang. Vision mamba: Efficient visual representation learning with bidirectional state space model. In Proceedings of ICML, 2024.
- [35] Yue Liu, Yunjie Tian, Yuzhong Zhao, Hongtian Yu, Lingxi Xie, Yaowei Wang, Qixiang Ye, Jianbin Jiao, and Yunfan Liu. Vmamba: Visual state space model. In Proceedings of NeurIPS, 2024.

- [36] Tao Huang, Xiaohuan Pei, Shan You, Fei Wang, Chen Qian, and Chang Xu. Localmamba: Visual state space model with windowed selective scan. CoRR, abs/2403.09338, 2024.
- [37] Xiaoyi Dong, Jianmin Bao, Dongdong Chen, Weiming Zhang, Nenghai Yu, Lu Yuan, Dong Chen, and Baining Guo. Cswin transformer: A general vision transformer backbone with cross-shaped windows. In Proceedings of IEEE CVPR, pages 12114–12124, 2022.
- [38] Sucheng Ren, Xingyi Yang, Songhua Liu, and Xinchao Wang. Sg-former: Self-guided transformer with evolving token reallocation. In Proceedings of IEEE ICCV, pages 5980–5991, 2023.
- [39] Chenglin Yang, Siyuan Qiao, Qihang Yu, Xiaoding Yuan, Yukun Zhu, Alan L. Yuille, Hartwig Adam, and Liang-Chieh Chen. MOAT: alternating mobile convolution and attention brings strong vision models. In Proceedings of ICLR, 2023.
- [40] Dongchen Han, Ziyi Wang, Zhuofan Xia, Yizeng Han, Yifan Pu, Chunjiang Ge, Jun Song, Shiji Song, Bo Zheng, and Gao Huang. Demystify mamba in vision: A linear attention perspective. In Proceedings of NeurIPS, 2024.
- [41] Wenhai Wang, Enze Xie, Xiang Li, Deng-Ping Fan, Kaitao Song, Ding Liang, Tong Lu, Ping Luo, and Ling Shao. PVT v2: Improved baselines with pyramid vision transformer. Comput. Vis. Media, 8(3):415–424, 2022.
- [42] Manjin Kim, Paul Hongsuck Seo, Cordelia Schmid, and Minsu Cho. Learning correlation structures for vision transformers. In Proceedings of CVPR, pages 18941–18951, 2024.
- [43] Ze Liu, Yutong Lin, Yue Cao, Han Hu, Yixuan Wei, Zheng Zhang, Stephen Lin, and Baining Guo. Swin transformer: Hierarchical vision transformer using shifted windows. In Proceedings of IEEE ICCV, pages 9992–10002, 2021.
- [44] Kaiming He, Georgia Gkioxari, Piotr Dollár, and Ross B. Girshick. Mask R-CNN. In Proceedings of ICCV, pages 2980–2988, 2017.
- [45] Tsung-Yi Lin, Priya Goyal, Ross B. Girshick, Kaiming He, and Piotr Dollár. Focal loss for dense object detection. In Proceedings of ICCV, pages 2999–3007, 2017.
- [46] Youngwan Lee, Jonghee Kim, Jeffrey Willette, and Sung Ju Hwang. Mpvit: Multi-path vision transformer for dense prediction. In Proceedings of CVPR, pages 7277–7286, 2022.
- [47] Jianyuan Guo, Kai Han, Han Wu, Yehui Tang, Xinghao Chen, Yunhe Wang, and Chang Xu. CMT: convolutional neural networks meet vision transformers. In Proceedings of IEEE CVPR, pages 12165–12175. IEEE, 2022.
- [48] Alaaeldin Ali, Hugo Touvron, Mathilde Caron, Piotr Bojanowski, Matthijs Douze, Armand Joulin, Ivan Laptev, Natalia Neverova, Gabriel Synnaeve, Jakob Verbeek, and Hervé Jégou. Xcit: Cross-covariance image transformers. In Proceedings of NeurIPS, pages 20014–20027, 2021.
- [49] Ali Hassani, Steven Walton, Jiachen Li, Shen Li, and Humphrey Shi. Neighborhood attention transformer. In Proceedings of CVPR, pages 6185–6194, 2023.
- [50] Ali Hatamizadeh, Hongxu Yin, Greg Heinrich, Jan Kautz, and Pavlo Molchanov. Global context vision transformers. In Andreas Krause, Emma Brunskill, Kyunghyun Cho, Barbara Engelhardt, Sivan Sabato, and Jonathan Scarlett, editors, Proceedings of ICML, volume 202, pages 12633–12646, 2023.
- [51] Alexander Kirillov, Ross B. Girshick, Kaiming He, and Piotr Dollár. Panoptic feature pyramid networks. In Proceedings of CVPR, pages 6399–6408, 2019.
- [52] Tete Xiao, Yingcheng Liu, Bolei Zhou, Yuning Jiang, and Jian Sun. Unified perceptual parsing for scene understanding. In Vittorio Ferrari, Martial Hebert, Cristian Sminchisescu, and Yair Weiss, editors, Proceedings of ECCV, volume 11209, pages 432–448. Springer, 2018.
- [53] Songlin Yang, Jan Kautz, and Ali Hatamizadeh. Gated delta networks: Improving mamba2 with delta rule. CoRR, abs/2412.06464, 2024.

- [54] Daniel Bolya, Cheng-Yang Fu, Xiaoliang Dai, Peizhao Zhang, and Judy Hoffman. Hydra attention: Efficient attention with many heads. In Leonid Karlinsky, Tomer Michaeli, and Ko Nishino, editors, Proceedings of ECCV, volume 13807, pages 35–49. Springer, 2022.
- [55] Zhuoran Shen, Mingyuan Zhang, Haiyu Zhao, Shuai Yi, and Hongsheng Li. Efficient attention: Attention with linear complexities. In Proceedings of WACV, pages 3530–3538, 2021.
- [56] Haoran You, Yunyang Xiong, Xiaoliang Dai, Bichen Wu, Peizhao Zhang, Haoqi Fan, Peter Vajda, and Yingyan Celine Lin. Castling-vit: Compressing self-attention via switching towards linear-angular attention at vision transformer inference. In Proceedings of CVPR, pages 14431–14442. IEEE, 2023.
- [57] Xiangxiang Chu, Zhi Tian, Bo Zhang, Xinlong Wang, and Chunhua Shen. Conditional positional encodings for vision transformers. In Proceedings of ICLR. OpenReview.net, 2023.
- [58] MMCV Contributors. MMCV: OpenMMLab computer vision foundation. <https://github.com/open-mmlab/mmcv>, 2018.
- [59] Hugo Touvron, Thibaut Lavril, and et al. Gautier Izacard. Llama: Open and efficient foundation language models. CoRR, abs/2302.13971, 2023.
- [60] Yutao Sun, Li Dong, Shaohan Huang, Shuming Ma, Yuqing Xia, Jilong Xue, Jianyong Wang, and Furu Wei. Retentive network: A successor to transformer for large language models. CoRR, abs/2307.08621, 2023.
- [61] Albert Gu and Tri Dao. Mamba: Linear-time sequence modeling with selective state spaces. CoRR, abs/2312.00752, 2023.
- [62] Daria Soboleva, Faisal Al-Khateeb, Robert Myers, Jacob R Steeves, Joel Hestness, and Nolan Dey. SlimPajama: A 627B token cleaned and deduplicated version of RedPajama, 2023.
- [63] Stephen Merity, Caiming Xiong, James Bradbury, and Richard Socher. Pointer sentinel mixture models. In Proceedings of ICLR, 2017.
- [64] Denis Paperno, Germán Kruszewski, Angeliki Lazaridou, Quan Ngoc Pham, Raffaella Bernardi, Sandro Pezzelle, Marco Baroni, Gemma Boleda, and Raquel Fernández. The LAMBADA dataset: Word prediction requiring a broad discourse context. In Proceedings of the 54th Annual Meeting of the Association for Computational Linguistics (ACL), 2016.
- [65] Peter Clark, Isaac Cowhey, Oren Etzioni, Tushar Khot, Ashish Sabharwal, Carissa Schoenick, and Oyvind Tafjord. Think you have solved question answering? try arc, the AI2 reasoning challenge. CoRR, abs/1803.05457, 2018.
- [66] Rowan Zellers, Ari Holtzman, Yonatan Bisk, Ali Farhadi, and Yejin Choi. Hellaswag: Can a machine really finish your sentence? In Proceedings of the 57th Conference of the Association for Computational Linguistics (ACL), pages 4791–4800. Association for Computational Linguistics, 2019.
- [67] Yonatan Bisk, Rowan Zellers, Ronan Le Bras, Jianfeng Gao, and Yejin Choi. PIQA: reasoning about physical commonsense in natural language. In Proceedings of AAAI, pages 7432–7439, 2020.
- [68] Keisuke Sakaguchi, Ronan Le Bras, Chandra Bhagavatula, and Yejin Choi. Winogrande: An adversarial winograd schema challenge at scale. In Proceedings of AAAI, pages 8732–8740, 2020.
- [69] Hugo Touvron, Matthieu Cord, Matthijs Douze, Francisco Massa, Alexandre Sablayrolles, and Hervé Jégou. Training data-efficient image transformers & distillation through attention. In Proceedings of ICML, volume 139, pages 10347–10357, 2021.
- [70] Zhaozhi Wang, Yue Liu, Yunfan Liu, Hongtian Yu, Yaowei Wang, Qixiang Ye, and Yunjie Tian. wheat: Building vision models upon heat conduction. CoRR, abs/2405.16555, 2024.
- [71] Yuwei Qiu, Kaihao Zhang, Chenxi Wang, Wenhan Luo, Hongdong Li, and Zhi Jin. Mbtaylorformer: Multi-branch efficient transformer expanded by taylor formula for image dehazing. In Proceedings of IEEE ICCV, pages 12756–12767, 2023.

## A Appendix

- **A.1 Entropy Analysis.** The mathematical proof and supporting lemmas of Theorem 1 and Theorem 2
- **A.2 Datasets and Experiment Details.** Training settings and datasets for all experiments.
- **A.3 Limitations.** The limitations of this work.
- **A.4 Related Work.** Related works about vision transformer and linear attention.

### A.1 Entropy Analysis

In this section, we use the Positive Sequence Entropy (PSE) [10] to connect the probability distribution with the sequence of query-key similarity (one row in the feature map). We first prove the  $\text{PSE}(\cdot)$  is concave. Then, we analysis the PSE of  $t$ -th row of the feature map,  $\mathbf{x} = (x_1, \dots, x_N)$ ,  $x_i = \mathbf{q}_t \mathbf{k}_i^\top$ , with query norm  $\|\mathbf{q}_t\|$  and single key norm  $\|\mathbf{k}_i\|$ .

**Lemma 1.**  $\text{PSE}(\cdot)$  is a concave function with respect to each of its variables separately.

*Proof.* We firstly introduce the positive sequence entropy (PSE) defined in PolaFormer [10] as follows,

$$\text{PSE}(\mathbf{x}) = \text{H}\left(\frac{\mathbf{x}}{S}\right) = -\sum_{i=1}^n \frac{x_i}{S} \log\left(\frac{x_i}{S}\right)$$

where  $S = \sum_{i=1}^n x_i$ . Additionally, we assume  $\{x_i\}$  is a set of independent random variables. Then, we explicitly formulate the partial derivatives of  $\text{PSE}(\mathbf{x})$  with respect to  $x_i$

$$P := \text{PSE}(\mathbf{x}) = -\sum_{i=1}^n \frac{x_i}{S} \log\left(\frac{x_i}{S}\right) \quad (20)$$

$$= -\sum_{i=1}^n \left( \frac{x_i}{S} \log(x_i) - \frac{x_i}{S} \log(S) \right) \quad (21)$$

$$= -\left( \sum_{i=1}^n \frac{x_i}{S} \log(x_i) - \log(S) \right) \quad (22)$$

$$= \log(S) - \sum_{i=1}^n \frac{x_i}{S} \log(x_i) \quad (23)$$

For simplicity, we consider the logarithm base to be arbitrary in our derivations. Then we have,

$$\frac{\partial S}{\partial x_m} = 1 \quad (24)$$

$$\frac{\partial P}{\partial x_m} = \frac{1}{S} - \left( -\frac{1}{S^2} \sum_{i=1}^n (x_i \ln(x_i)) + \frac{1}{S} (1 + \ln(x_m)) \right) \quad (25)$$

$$= \frac{1}{S^2} \sum_{i=1}^n (x_i \ln(x_i)) - \frac{1}{S} \ln(x_m) \quad (26)$$

$$= \frac{1}{S^2} \left( \sum_{i=1}^n x_i \ln(x_i) - \sum_{i=1}^n x_i \ln(x_m) \right) \quad (27)$$

$$= \frac{1}{S^2} \sum_{i=1}^n x_i (\ln(x_i) - \ln(x_m)) \quad (28)$$

Due to the positiveness of  $\frac{1}{S^2}$ , which does not affect the signal of  $\frac{\partial P}{\partial x_m}$ , the second-order partial derivative is calculated on the series component in Eq. (28).

$$\frac{\partial^2 P}{\partial x_m^2} \sim \frac{\partial^2}{\partial x_m^2} \left( \sum_{i=1}^n x_i (\ln(x_i) - \ln(x_m)) \right) \quad (29)$$

$$= (1 + \ln(x)) - \left( \frac{\sum x_i}{x_m} + \ln(x_m) \right) \quad (30)$$

$$= 1 - \frac{\sum x_i}{x_m} \leq 0 \quad (31)$$

Therefore,  $\text{PSE}(\cdot)$  is a concave function of  $x_m$ .  $\square$

**Theorem (Query Norm Dynamic Entropy Reduction).** Consider a sequence  $\mathbf{x} = (x_1, \dots, x_N)$  and let  $\Phi : (-\infty, +\infty) \mapsto [0, +\infty)$  a spiky function serving to reducing the PSE through mapping each  $x_i$ . In softmax normalization, where  $\Phi(\cdot) = \exp(\cdot)$ , existing a constant value  $c_0$  satisfying:

For  $c > c_0$ , we have

$$\text{PSE}(\Phi(c\mathbf{x})) < \text{PSE}(\Phi(\mathbf{x}))$$

**Proof.** In the following derivation, we use the Positive Sequence Entropy (PSE) [10] to connect the softmax self-attention with  $\text{PSE}(\cdot)$ . Based on the Lemma 1 of  $\text{PSE}(\mathbf{x})$ , we investigate the probability distribution generated from one single query vector and a series of key vectors with PSE, analyzing how  $\text{PSE}(\mathbf{x})$  varying with query norm with softmax.

Assuming  $\mathbf{q}$  is a directional fixed vector with norm  $c$ , i.e.,  $\mathbf{q}_t = c_t \cdot d(\mathbf{q}_t)$ , we only consider the relation between PSE and  $c_t$ . Then, we have the following two propositions:

**Proposition 1.** *Softmax attention is query norm-aware.*

*Proof.* Without loss of generality, we assume the sum of the positive sequence have,  $\sum_{i=1}^N \Phi(x_i) = 1$ , and directly set query norm as a scaler  $c \in \mathbb{R}$ . Then, the PSE of  $\mathbf{x}$  degraded into Shannon entropy as,

$$\begin{aligned} \text{PSE}(\Phi(\mathbf{x})) &= H(\Phi(\mathbf{x})) \\ &= - \sum_{i=1}^N \Phi(x_i) \log(\Phi(x_i)) \end{aligned}$$

When query norm varies, the PSE is,

$$\begin{aligned} S_c &= \sum_{i=1}^N \Phi(cx_i) = \sum_{i=1}^N \Phi(x_i)^c = \|\Phi(\mathbf{x})\|_c^c \\ \text{PSE}(\Phi(c\mathbf{x})) &= \text{PSE}(\Phi(\mathbf{x})^c) = \log(S_c) - \sum_{i=1}^N \frac{\Phi(x_i)^c}{S_c} \log(\Phi(x_i)^c) \\ &= c \log(\|\Phi(\mathbf{x})\|_c) - c \sum_{i=1}^N \frac{\Phi(x_i)^c}{\|\Phi(\mathbf{x})\|_c^c} \log(\Phi(x_i)) \end{aligned}$$

Due to the definition of  $L_p$  norm,  $\lim_{p \rightarrow \infty} \|x\|_p = x_{max}$ , and  $x_i \in [0, 1]$ , we have  $\|x\|_p \leq x_{max}$  for  $p > 1$ . Therefore,

$$c \log(\|\Phi(\mathbf{x})\|_c) - c \sum_{i=1}^N \frac{\Phi(x_i)^c}{\|\Phi(\mathbf{x})\|_c^c} \log(\Phi(x_i)) \leq c \log(\Phi(x_{max})) - c \sum_{i=1}^N \left(\frac{\Phi(x_i)}{\Phi(x_{max})}\right)^c \log(\Phi(x_i))$$

When  $c \rightarrow +\infty$ ,  $\left(\frac{\Phi(x_i)}{\Phi(x_{max})}\right)^c \rightarrow 0$  for all  $x_i \neq x_{max}$ :

$$\begin{aligned} \lim_{c \rightarrow +\infty} c \log(\Phi(x_{max})) - c \sum_{i=1}^N \left(\frac{\Phi(x_i)}{\Phi(x_{max})}\right)^c \log(\Phi(x_i)) \\ = c \log(\Phi(x_{max})) - c \log(\Phi(x_{max})) = 0 \end{aligned}$$

Therefore, because PSE is positive, there exists  $c_0$ , for all  $c > c_0$ ,  $\text{PSE}(\Phi(c\mathbf{x})) < \text{PSE}(\Phi(\mathbf{x}))$   $\square$

Consequently, the Proposition 1 proves the theorem softmax attention is query norm aware with a dynamic control on entropy reduction.  $\blacksquare$

Similar to linear attention, we continue with the case in previous linear attention. For most of the kernel function in linear attention, such as ReLU, SiLU or 1+ELU, there exists

**Proposition 2.** *Linear attention is query norm-unaware.*

*Proof.* In linear attention, we have  $\Phi(x_m) = \phi(\mathbf{q})\phi(\mathbf{k}_m)^\top$  and  $\Phi(cx_m) = c\Phi(x_m)$ , thus the PSE of linear attention can be written as,

$$\begin{aligned}
 S &= \sum_{m=1}^N \Phi(x_m) \\
 \text{PSE}_{\text{linear}}(\mathbf{x}) &= \log(S) - \sum_{i=1}^N \frac{\Phi(x_i)}{S} \log(\Phi(x_i)) \\
 \text{PSE}_{\text{linear}}(c\mathbf{x}) &= \log(c) + \log(S) - \sum_{i=1}^N \frac{c\Phi(x_i)}{c \cdot S} (\log(\Phi(x_i)) + \log(c)) \\
 &= \log(c) + \log(S) - \sum_{i=1}^N \frac{c\Phi(x_i)}{c \cdot S} (\log(\Phi(x_i))) - \sum_{i=1}^N \frac{c\Phi(x_i)}{c \cdot S} \log(c) \\
 &= \log(S) - \sum_{i=1}^N \frac{c\Phi(x_i)}{c \cdot S} (\log(\Phi(x_i))) + \log(c) - \sum_{i=1}^N \frac{c\Phi(x_i)}{c \cdot S} \log(c) \\
 &= \text{PSE}_{\text{linear}}(\mathbf{x})
 \end{aligned}$$

□

**Theorem (Kernel Function Design).** Consider a sequence  $\mathbf{x} = (x_1, \dots, x_n)$ , calculated by  $\mathbf{q}\mathbf{k}_i^\top$ . Given a spiky function  $\Phi(\cdot)$  satisfying that  $\Phi : (-\infty, +\infty) \mapsto [0, +\infty)$  is a differentiable function with  $\Phi'(x) > 0$  and  $\Phi''(x) > 0$ . Then,  $\text{PSE}(\Phi(\cdot))$  is a norm aware concave function and a decreasing function for a great query norm.

*Proof.* According to Eq. (31) in Lemma 1, we know that Eq.(23) is an increasing function and the PSE is decreasing with each great enough  $x_m$ . Connecting the Proposition 1 with the properties of convex functions, we can conclude that the spiky function  $\Phi(\cdot)$  must satisfy both  $\Phi' > 0$  and  $\Phi'' > 0$ , additionally, to preserve the query norm awareness,  $\Phi(\cdot)$  also should satisfy  $\frac{\Phi(cx)}{\Phi(x)}$  is not constant. □

## A.2 Datasets and Experiment Details

**Image Classification.** In this task, we train all of our models with AdamW optimizer for 320 epochs, including 20 epochs for linear warm-up. The basic learning rate is set to 0.001 for 128 micro batchsize and 1024 global batchsize. The training framework is developed on the top of the official DeiT implementation. Additionally, we use CPE [57] to serve as the positional encoding. When mapping each  $d(\mathbf{x})$ , we set  $f(x) = \frac{\pi}{4} \tanh(x)$  to make the cosine function only inhibits the directions with opposite signals.

**Object Detection and Segmentation.** We further conducted comprehensive experiments on the object detection task using the COCO dataset [20], which contains 118K training images and 5K validation images annotated with 80 object categories. We use our model as backbone with pretrained weights on ImageNet-1K. We conduct the experiments following the *mmcv-detection* [58] project. The model are trained under both  $1 \times$  (12 epochs) and  $3 \times$  (36 epochs). We use the AdamW optimizer with 0.0001 learning rate, 0.0001 weight decay and “step” policy.

**Semantic Segmentation.** We conduct the semantic segmentation of ADE20K dataset [21]. This widely adopted dataset comprises 25,000 densely annotated images depicting complex real-world environments with rich contextual interactions between objects and their spatial configurations. We employ the pretrained NALFormer models on two representative segmentation models, SemanticFPN and UperNet. The experiment is conducted based on *mmcv-segmentation* [58]. The training iteration is set to 40000 for SemanticFPN models and 160000 for UperNet models. All models are trained using AdamW optimizer with 0.0001 learning rate and 0.001 weight decay.

**Language Modeling.** We compare NALFormer with several baseline models, including Transformer++ [59], Gated Linear Attention [15], RetNet [60], Mamba [61], DeltaNet [8] and Gated DeltaNet [53]. Each model is pretrained on the subset of the SlimPajama dataset [62]. We train our

model from scratch with parameter sizes of 340M on 15B tokens with a batch size of 0.5M tokens and test it on common-sense reasoning tasks, which includes WikiText [63], LAMBADA [64], ARC-easy [65], ARC-challenge [65], HellaSwag [66], PiQA [67] and WinoGrande [68]. All downstream tasks are conducted based on *lm-evaluation-harness*. We test throughput of the baseline models on a single A6000 GPU.

### A.3 Limitations

While this work validates the efficacy of NaLaFormer across diverse vision-language tasks, we anticipate that its linear self-attention architecture holds significant potential for other cross-modality applications, such as text-to-image and text-to-video generation. However, direct evaluation in such contexts presents considerable challenges, primarily due to the substantial computational complexity associated with training diffusion models from scratch. Future efforts will actively pursue these promising directions and develop novel strategies to accelerate training efficiency, thereby enabling scalable deployment of NALAFormer in complex generative modeling tasks.

### A.4 Related Work

**Vision Transformer.** The success of the Transformer architecture [1] in natural language processing (NLP), particularly its self-attention mechanism for modeling long-range dependencies, has catalyzed its adoption in computer vision (CV). The vision transformer [2] marked a paradigm shift by discarding convolutions entirely. The vision transformer partitions images into patches, linearly embeds these patches into sequential tokens, and processes them through a pure Transformer encoder. Nevertheless, the quadratic computational complexity inherent in self-attention mechanisms incurs substantial computational overhead, rendering ViT training computationally intensive. Existing researches have proposed multiple strategies to enhance ViT’s efficiency. For instance, DeiT [69] achieves data-efficient training through knowledge distillation, whereas the Swin Transformer [43] employs shifted window mechanisms to balance local feature extraction with global context modeling while maintaining linear complexity. These advancements have established Transformer-based architectures as fundamental frameworks for visual tasks, effectively bridging the methodological divide between NLP-oriented architectures and CV’s inherent geometric constraints. However, these improvements primarily address architectural adaptations rather than resolving the fundamental limitations of softmax-based attention mechanisms, thereby retaining significant training costs. Recent studies have explored alternative paradigms for visual representation learning to mitigate these constraints. Building on sequential image processing principles, several approaches employ state space models (SSMs) for patch encoding. Notably, VMamba [35, 36] leverages SSM-based encoding through raster-scan ordering to extract hierarchical features while preserving the theoretical guarantee of linear computational complexity inherent to SSMs. In addition, VHeat [70] reconceptualizes image understanding through thermodynamic simulations, modeling image patches as heat sources, and analyzing thermal conduction processes, reducing the complexity to  $\mathcal{O}(N^{1.5})$  through discrete cosine transforms (DCT) and inverse DCT operations.

**Linear Attention.** Linear attention employs kernel-based similarity approximation to circumvent the  $\exp(\mathbf{qk}^\top)$  in standard softmax attention. The foundational work [3] introduces a linear separable kernel  $\phi(\cdot)$  as an alternative to the exp operator, exploiting the associative property of matrix multiplication to reduce computational complexity from  $\mathcal{O}(N^2)$  to  $\mathcal{O}(N)$ . Subsequent variants adopt this Softmax-free paradigm with diverse kernel functions, including ReLU [5, 4], 1+ELU [3] and SiLU [8, 6]. Furthermore, to enhance position awareness, Cosformer [17] integrates ReLU with Ptolemy’s theorem, incorporating locality inductive biases through feature map re-weighting while empirically enforcing non-negativity constraints. Beyond kernel design, recent studies focus on preserving the spikiness property inherent in softmax attention. Hedgehog [9] and MB-TaylorFormer [71] employ series expansions to approximate the exp function, while FLatten Transformer [5] and PolaFormer [10] utilize power functions to sharpen attention distributions. Notably, lightning attention [16] combines SiLU kernels with a gate mechanism, achieving scalability up to 456B parameters [6]. In autoregressive architectures, linear attention enables RNNs parallelization through unidirectional encoding. Gated Linear Attention enhances this capability via data-dependent gating on  $\mathbf{K}^\top \mathbf{V}$  hidden states, demonstrating superior performance in length generalization and recall-intensive tasks. However, current kernel functions exhibit performance degradation compared to standard softmax attention. Our analysis reveals significant information loss arising from query norm cancellation during linear attention normalization, necessitating norm-preserving kernel designs – a challenge addressed in subsequent sections.